arXiv:1107.5571v1 [cond-mat.str-el] 27 Jul 2011

Probing the Two-Fluid Behavior in $\mathrm{CeIn}_{3-x}\mathrm{Sn}_x$ by Electron Spin Resonance

E. M. Bittar,[1, 2, *] C. Adriano,[1] C. Giles,[1] C. Rettori,[1, 3] and P. G. Pagliuso[1]

[1] *Instituto de Física "Gleb Wataghin", UNICAMP, 13083-859, Campinas, SP, Brazil*

[2] *Laboratório Nacional de Luz Síncrotron, C. P. 6192, 13083-970, Campinas, SP, Brazil*

[3] *Centro de Ciências Naturais e Humanas, Universidade Federal do ABC, 09210-170, Santo André, SP, Brazil*

(Dated: July 28, 2011)

The $\mathrm{CeIn}_{3-x}\mathrm{Sn}_x$ cubic heavy fermion system presents an antiferromagnetic transition at $T_N = 10$ K, for $x = 0$, that vanishes continuously upon Sn substitution at $x_c \approx 0.7$. In the vicinity of $T_N \to 0$ the system shows non-Fermi liquid behavior due to antiferromagnetic critical fluctuations. We show that Gd^{3+} electron spin resonance (ESR) probes a change in the character of the Ce $4f$ electron as a function of Sn substitution which follows the description of the two-fluid model for heavy fermions. Besides, some indication for a local class of quantum critical point for this system is discussed.

PACS numbers: 71.27.+a, 74.40.Kb, 76.30.-v

Heavy fermion (HF) system have shown to the scientific community interesting physical phenomena like antiferromagnetism (AFM), superconductivity (SC) [1] and non-Fermi liquid (NFL) behavior in the vicinity of quantum instabilities [2]. However, the evolution from the high-T unscreened localized f electrons to itinerant heavy quasiparticles at low-T is still an open question in condensed matter physics. The description of these HF materials stands on the Kondo lattice model [1] in which there are three important energy scales: the crystalline electric field (CEF) splitting, the characteristic temperature T^* and the single impurity Kondo temperature T_K. The latter is related to the screening of local moments by the conduction electrons due to the Kondo effect. T^* represents the crossover between a lattice of Kondo impurities to a coherence state where the hybridization becomes a global process and is related to the Ruderman–Kittel–Kasuya–Yosida (RKKY) exchange interaction, since it corresponds to the nearest-neighbor intersite coupling, which is mediated by the conduction electrons [3]. Recently, the interplay between these energies scales led to a two-fluid description of the Kondo lattice, which was later generalized to a standard phenomenological model [6] that can probably substitute the Doniach model for HF systems. The two-fluid model states that below T^* the weakly interacting local moments Kondo centers, hereafter named the Kondo-gas phase (KGP), might coexist with a HF liquid of itinerant moments, the Kondo-liquid phase (KLP) [4, 5]. In the low-T regime one can attribute an order parameter $[1-f(T/T^*)]$ to the KGP and $f(T/T^*)$ to the partial condensed KLP, so the $4f$ electron might have two components, specially when quantum critical behavior is present. Away form such quantum critical point (QCP) the HF ground state is expected to be described only by the KLP $[f(T/T^*) = 1]$ or the KGP $[f(T/T^*) = 0]$ [4, 5]. Although previous nuclear magnetic resonance [7] and Raman [8] studies seemed to be consistent with the two-fluid model in HF materials, additional and more conclusive microscopic experimental evidence for such behavior is still highly desirable.

The cubic HF system $\mathrm{CeIn}_{3-x}\mathrm{Sn}_x$ is an interesting series to study the correlations between T_K and T^*. For $x = 0$ the compound is AFM with $T_N = 10$ K and by Sn substitution, $T_N \to 0$ continuously up to $x_c \approx 0.65$ [9, 10]. This system resembles the behavior of CeIn_3 under pressure P where a SC state emerges at $P_c \approx 25$ kbar with critical temperature $T_c \approx 0.15$ K and $T_N \to 0$ [11]. In the vicinity of P_c and x_c both systems show NFL behavior suggesting that AFM critical fluctuations are present. Recently the analysis of the magnetic contribution to the specific heat in CeIn_3 showed that the magnetic fluctuations in this material are effectively 2D [12]. Indeed an almost linear dependence of $T_N(x)$ is seen for $\mathrm{CeIn}_{3-x}\mathrm{Sn}_x$ [10], in contrast to what is predicted by the 3D spin density wave (SDW) theory and it cannot be associated to disorder effects [13]. The reported scenario for the P or Sn substitution driven QCP were somewhat conflicting. For $\mathrm{CeIn}_{3-x}\mathrm{Sn}_x$ it was used a SDW description of criticality based on critical exponents analysis of a 3D-AFM [13, 14]. In the SDW QCP the $4f$ moments are delocalized in the AFM state and no change of the Fermi surface (FS) is observed across the QCP [2]. However, in a local class of QCP the $4f$ electrons remain localized in the magnetically ordered phase and there is an abrupt change of the FS volume at the QCP [2]. For the CeIn_3 under P a local QCP was proposed due to a FS volume change observed in de-Haas-van-Alphen measurements [15].

In order to clarify the contradictory nature of the QCPs of CeIn_3, we study the evolution of the Gd^{3+} ESR signal in the $\mathrm{CeIn}_{3-x}\mathrm{Sn}_x$ system through its QCP. Since Ce^{3+} ESR signal is silent, we chose Gd^{3+} as a probe because it is almost a pure S-state, so its total angular momentum is mainly due to spin and is weakly perturbed by CEF effects. Nuclear quadrupolar resonance measurements were carried out for the P-induced QCP [16] but to the best of our knowledge no systematic reports on microscopic studies on the Sn substitution QCP were reported. Our Gd^{3+} ESR results show a change in the character of the Ce $4f$ electron as a function of

Sn substitution which follows the description of the HF two-fluid model. Although it is difficult to assert definitively what is the actual class of the QCP, the evidence for some remaining localization character of the $4f$ electrons close to the QCP, in the AFM phase, indicate that $\mathrm{CeIn}_{3-x}\mathrm{Sn}_x$ is actually similar to the picture given by the P-driven QCP in CeIn_3.

Single and/or polycrystals of Gd doped $\mathrm{CeIn}_{3-x}\mathrm{Sn}_x$ are synthesized by (In,Sn)-flux and/or arc melting, respectively. As a reference compound, Gd doped $\mathrm{LaIn}_{3-x}\mathrm{Sn}_x$ alloys were also grown and studied [17]. The actual Sn concentrations are obtained measuring the cubic lattice parameter and assuming a linear increase wtih Sn (Vegard law) [10]. From the Curie-Weiss law fitting of the low-T magnetic susceptibility data the Gd doping concentration is obtained and its values are shown in Table I. See details in Ref. 18.

Figure 1(a) shows selected ESR (X-band) powder spectra at ~ 10 K of Gd^{3+} in $\mathrm{CeIn}_{3-x}\mathrm{Sn}_x$. Except for $x = 0$ the ESR spectra consist of a single Dysonian resonance, consistent with the ESR for localized magnetic moments in a metallic host with a skin depth smaller than the size of the used particles. By fitting the lineshape to the appropriate admixture of absorption and dispersion Lorentzian derivatives we obtain the g value and linewidth ΔH of the resonances. Particulary for $x = 3$ we show that there is no appreciable difference in the resonance between single and polycrystalline samples. The solid lines are the best fit to the observed resonances and the obtained g shift Δg (relative to $g = 1.993$ in insulators) are presented in Table I. For Gd^{3+} in CeIn_3 the ESR spectrum shows the typical fine-structure features for powder samples [19], with a main line at $H \sim 3.45$ kOe, associated with the $1/2 \leftrightarrow 1/2$ transition. A previous report in this compound, using the spin Hamiltonian $H = g\mu_B \mathbf{H}\cdot\mathbf{S} + (1/60)b_4(O_4^0 + 5O_4^4) + J_{fs}\mathbf{S}\cdot\mathbf{s}$ [20], extracted the crystal field parameter $b_4 = 90(5)$ Oe [21]. The ΔH T-dependence is shown in Fig. 1(b). The linear dependence of the ΔH is fitted to the expression $\Delta H - \Delta H_0 = bT$. The values for ΔH_0 (residual linewidth) and b (thermal broadening) are presented in Table I. The relatively high ΔH_0 values for $0 < x < 3$ are probably due to of unresolved CEF and disorder introduced by the In-Sn substitution. For $\mathrm{Ce}_{0.996}\mathrm{Gd}_{0.004}\mathrm{In}_3$ the ΔH T-dependance for the main line is analyzed. A deviation from the linear dependence of ΔH at low-T is seen for $x = 1.5$ which is related to short range Gd-Gd interaction. Within the accuracy of the measurements, the g and b values are Gd concentration independent for $y < 2.0\%$. Therefore, bottleneck and dynamic effects can be disregarded [22].

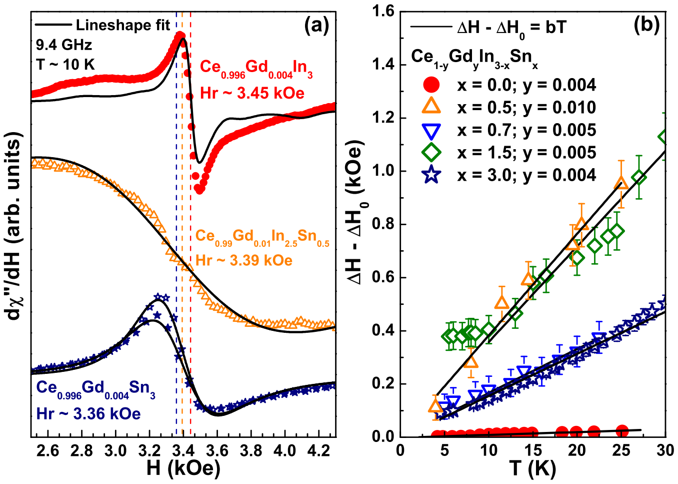

FIG. 1: Gd^{3+} ESR in $\mathrm{Ce}_{1-y}\mathrm{Gd}_y\mathrm{In}_{3-x}\mathrm{Sn}_x$ for $y \sim 0.5\%$: (a) selected X-band (9.4 GHz) ESR powder spectra of Gd^{3+}, at $T \approx 10$ K. The solid lines are the Dysonian line shape analysis. The vertical dashed lines are the resonance field H_r for each spectrum. (b) T-dependence of the ESR linewidth. The solid lines are the best fit to $\Delta H - \Delta H_0 = bT$. The closed symbols identify the single crystalline samples and the open ones the polycrystals.

TABLE I: Experimental parameters for Gd^{3+} diluted in $\mathrm{Ce}_{1-y}\mathrm{Gd}_y\mathrm{In}_{3-x}\mathrm{Sn}_x$. The values of γ are taken from Ref. 10.

Gd^{3+} in	Gd y	Δg	ΔH_0 [Oe]	b [Oe/K]	γ [mJ/mol K^2]
CeIn_3	0.004	-0.023(5)	120(5)	0.1(1)	130
$\mathrm{CeIn}_{2.5}\mathrm{Sn}_{0.5}$	0.010	+0.007(10)	825(45)	38(3)	730(50)
$\mathrm{CeIn}_{2.3}\mathrm{Sn}_{0.7}$	0.005	+0.027(10)	820(25)	15(5)	750(50)
$\mathrm{CeIn}_{1.5}\mathrm{Sn}_{1.5}$	0.005	+0.140(10)	650(60)	30(5)	250(20)
CeSn_3	0.004	+0.027(5)	150(5)	16(1)	73

In metals, the exchange interaction $J_{fs}(q)\mathbf{S}\cdot\mathbf{s}$ between a Gd^{3+} localized $4f$ electron spin ($\mathbf{S}$) and the conduction electrons (ce) spin ($\mathbf{s}$) of the host metal yields an ESR Δg (Knight shift) given by [23]

$$\Delta g = J_{fs}(0)\eta_{F_s}, \tag{1}$$

where $J_{fs}(0)$ is the effective exchange interaction parameter between the Gd^{3+} $4f$ local moments and the s-like ce in the absence of ce's momentum transfer ($q = |\mathbf{k}-\mathbf{k}'| = 0$) [24]. η_{F_s} is the bare density of states for one spin direction at the Fermi level for the s-like ce.

Another outcome of the exchange interaction is a thermal broadening of ΔH b (Korringa rate) given by [23]

$$b = \frac{\pi k_B}{g\mu_B}\left\langle J_{fs}^2(q)\right\rangle_F \eta_{F_s}^2 = \frac{\pi k_B}{g\mu_B}\frac{\left\langle J_{fs}^2(q)\right\rangle_F}{J_{fs}^2(0)}\Delta g^2, \tag{2}$$

where $\pi k_B/g\mu_B = 2.34\times10^4$ Oe/K and $\langle J_{fs}^2(q)\rangle_F$ is the square of the effective exchange interaction constant in the presence of ce's momentum transfer, averaged over the Fermi surface (FS) [24].

We now analyze separately the experimental ESR data for each synthesized compound. Details of the calculations can be found in the supplemental material [18].

$\underline{x = 0}$: In the absence of strong electron-electron exchange interaction and assuming that $\langle J^2_{fs}(q)\rangle^{1/2}_F = J_{fs}(0)$, i.e., the effective exchange interaction is isotropic over the FS, one expects $b \approx 12(5)$ Oe/K from Eq. 2, using the experimental Δg. This value is much larger than that measured experimentally $b = 0.1(1)$ Oe/K (Fig. 1b). Thus, the approximations that the relaxation does not depend on q and that it is due to the contribution of a single conduction s-like band are not adequate. Since Δg is negative a relaxation via a single s band is not plausible because J_{fs} would be of atomic-like and positive. Thus, for $\Delta g < 0$, contributions coming from covalent-like (negative) exchange interaction between the Gd^{3+} 4f-electron and *ce*-bands (p- or f-bands) must take place in the relaxation process [23]. However, multiple band would lead to a Korringa rate larger than the one expected from the Δg [25], contrary to what is observed for Gd^{3+} in CeIn$_3$. Therefore, a strong q dependent effective exchange interaction parameter $J_{fp}(q)$ or $J_{ff}(q)$ is expected in this compound. For CeIn$_3$ the local magnetic moment of Ce is compensated by the *ce* sea due to the Kondo effect. However, when Gd^{3+} substitutes the Ce ions there is a strong Coulomb repulsion potential that decreases the local density of states at the Gd^{3+} site, hence decreasing the Korringa rate (Eq. 2). Theoretical calculations have already showed that the spin relaxation rate of a well-defined magnetic moment in the neighborhood of a fluctuating valence ion decreases in relation to the relaxation rate of a undoped metal [26]. Indeed a much larger Korringa rate $b = 16(1)$ Oe/K was measured in Gd doped LaIn$_3$ [21]. This has also been observed for Gd in CePd$_3$ which presented an ESR ΔH thermal broadening five times smaller than in LaPd$_3$ [27]. Besides, the observation of fine-structure features in the spectrum (Fig. 1(a)) even up to room-T without narrowing effects [23] (not shown) suggests a low local density of states at the Gd^{3+} site. Another consequence of the screening of Ce^{3+} magnetic moment by the *ce* is observed in the relaxation ΔH (Fig. 1(b)). The Gd^{3+} resonance does not sense the internal field caused by the AFM transition. No change in the relaxation nor in the resonance field is observed below $T_N = 10$ K.

From the considerations above we can assume that the interaction of the Gd^{3+} 4f local moment is mainly with the Ce f-like *ce*. Using Eqs. 1 and 2 as $\Delta g = J_{ff}(0)\eta_{F_f}$ and $b = \pi k_B/g\mu_B\langle J^2_{ff}(q)\rangle_F\eta^2_{F_f}$, respectively, we calculate $J_{ff}(0) = -0.8(1)$ meV and $\langle J^2_{ff}(q)\rangle^{1/2}_F = 0.07(1)$ meV.

For these calculations, the values for the total bare density of states are obtained assuming a free *ce* gas model $\gamma = (2/3)\pi^2 k^2_B\eta_F$ given in Table I (see details in Ref. 18).

$\underline{x = 0.5}$: By substituting 16.67% of In by Sn, $x = 0.5$, T_N drops to ~ 1.3 K [10], very close to x_c. We also see Δg going from a relatively large negative to a very small $\simeq 7(10) \times 10^{-3}$ positive value. Considering that $\langle J^2_{fs}(q)\rangle^{1/2}_F = J_{fs}(0)$, from Eq. 2 we get $b_{cal} \ll b_{exp}$. It is clear that for Ce$_{0.990}$Gd$_{0.010}$In$_{2.50}$Sn$_{0.50}$ multiband effects are now present [25]. This is expected once Sn substitution hybridizes the localized Ce^{3+} 4f electrons turning them into itinerant s-like *ce* band. So, for $x = 0.5$ the Gd^{3+} resonance relaxes via contribution of the Ce 4f itinerant s- and localized f-like *ce* bands. If we admit $J_{ff}(0)^{x=0} = J_{ff}(0)^{x=0.5}$ it is possible to calculate $J_{fs}(0)$ and the density of states of each band since $\eta^{x=0.5}_{F_f} = \eta_{F_f^{itinerant}} + \eta_{F_f^{localized}}$. Solving the system of three equations $\eta^{x=0.5}_{F_f} = \eta_{F_f^{it}} + \eta_{F_f^{loc}}$, $\Delta g = J_{fs}(0)\eta_{F_f^{it}} + J_{ff}(0)\eta_{F_f^{loc}}$ and $b = \pi k_B/g\mu_B[J^2_{fs}(0)\eta^2_{F_f^{it}} + J^2_{ff}(0)\eta^2_{F_f^{loc}}]$, we obtain $J_{fs}(0) = 0.3(1)$ meV, $\eta_{F_f^{itinerant}}$ and $\eta_{F_f^{localized}}$ 115(10) and 40(5) states/(eV mol spin), respectively. So, naively, this result indicates a weight of 74% of the Ce f-electrons become itinerant upon $x = 0.5$ Sn substitution while the other 26% remains localized. One may argue that the multiband effects would be in fact due to the presence of s electrons arisen from a weaken Kondo interaction at the Ce^{3+} site or by the addition of new electrons. However, small Sn substitution increases the *ce* attractive potential [26] and does not profoundly change the density of states, as seen in LaIn$_{3-x}$Sn$_x$ [17, 28], favoring the interpretation of a delocalization of the Ce f-electrons.

$\underline{x = 0.7}$: For Gd^{3+} in CeIn$_{2.3}$Sn$_{0.7}$ the system is in the vicinity of the QCP and Eq. 2, assuming $\langle J^2_{fs}(q)\rangle^{1/2}_F = J_{fs}(0)$, predicts $b_{cal} \approx b_{exp}$. Therefore, we can consider a single s-like *ce* band with no q dependance in the analysis of the resonance in this material. Hence from Eq. 2 and considering $\langle J^2_{fs}(q)\rangle^{1/2}_F = J_{fs}(0)$, we find $J_{fs}(0) = 0.2(1)$ meV, similar to value encountered for $x = 0.5$.

$\underline{x = 1.5}$: The Δg value observed gives $b_{cal} \gg b_{exp}$ by Eq. 2 (assuming $\langle J^2_{fs}(q)\rangle^{1/2}_F = J_{fs}(0)$). So in this case q dependance is present and $\langle J^2_{fs}(q)\rangle^{1/2}_F \neq J_{fs}(0)$. We calculate $J_{fs}(0) = 2.6(2)$ meV and $\langle J^2_{fs}(q)\rangle^{1/2}_F = 0.7(1)$ meV.

$\underline{x = 3}$: From Eq. 2, using $\langle J^2_{fs}(q)\rangle^{1/2}_F = J_{fs}(0)$, we get $b_{cal} \approx b_{exp}$, i.e., multiband and q dependance effects of the exchange interaction may be neglected. Thus, we estimate $J_{fs}(0) = 1.7(1)$ meV.

The derived effective exchange interaction parameters from the analysis above are summarized in Table II. Due to the suppositions and approximations considered in the calculations, the numerical values must be taken with care. However, it does not invalidate the qualitative microscopic description probed by ESR.

The nonmagnetic analog system LaIn$_{3-x}$Sn$_x$ is composed of SC Pauli paramagnets [28] and Gd^{3+} doped ESR measurements in these compounds showed that the Δg

TABLE II: Derived effective exchange interaction parameters for Gd^{3+} diluted in $CeIn_{3-x}Sn_x$.

Gd^{3+} in	$J_{fs}(0)$ [meV]	$\langle J^2_{fs}(q)\rangle^{1/2}_F$ [meV]	$\lvert J_{ff}(0)\rvert$ [meV]	$\langle J^2_{ff}(q)\rangle^{1/2}_F$ [meV]
$CeIn_3$			0.8(1)	0.07(1)
$CeIn_{2.5}Sn_{0.5}$	0.3(1)		0.8(1)	
$CeIn_{2.3}Sn_{0.7}$	0.2(1)			
$CeIn_{1.5}Sn_{1.5}$	2.6(2)	0.7(1)		
$CeSn_3$	1.7(1)			

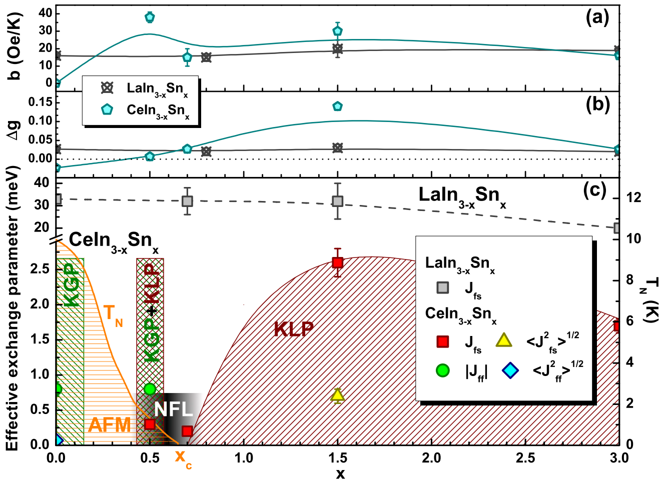

FIG. 2: (a) Linewidth thermal broadening b, (b) g shift (the dotted line mark $\Delta g = 0$) and (c) effective exchange interaction parameter evolution of Gd^{3+} ESR in $CeIn_{3-x}Sn_x$ as a function of x. The data for the $LaIn_{3-x}Sn_x$ compounds are taken from Ref. 17. The T_N evolution and the NFL region in the vicinity of the critical Sn concentration x_c are also seen [10]. For $CeIn_{3-x}Sn_x$ one can identify the presence of only the local moment weakly interacting KGP at $x = 0$ and the entangled KLP for $x \geq 0.7$, since only a single band effective exchange interaction is probed in each case. At $x = 0.5$, near the QCP, Gd^{3+} ESR probes that Ce f-electron has two components as in the two-fluid description of HF systems [4, 5]. The shaded areas and spline lines are guides to the eyes.

and b are not strongly changed by Sn substitution [17]. The Gd^{3+} resonance relaxation in these alloys is always via a single s-like ce band and $J_{fs}(0)$ is q independent, slightly decreasing with increasing x (Fig. 2) [17].

For the $CeIn_{3-x}Sn_x$ compounds the evolution of the Gd^{3+} ESR with Sn substitution is not as straightforward as in the reference. The b and Δg values profoundly change as a function of x (Figs. 2(a) and 2(b)). As we have seen, for $CeIn_3$ there is no exchange interaction between Gd^{3+} and the s-like ce. This due to the Kondo effect that creates an attractive potential for these s-like ce at the Ce sites. In this case the Gd^{3+} ESR relaxes only via a f-like localized ce band, i.e., it probes only a KGP, $f(T/T^*) = 0$. This attest that the Ce $4f$ electrons in $CeIn_3$ are strongly localized under high Kondo screening. As the systems approaches the QCP ($x = 0.5$), but still presenting AFM order, we observe the appearance of multiband effects in the resonance since hybridization effects, due to Sn substitution, turns some of these localized $4f$ electrons into itinerants, giving rise to a s-like ce band. For this alloy the $4f$ electrons coexists in the KGP and KLP, as in the two-fluid description of HF [4, 5]. In the vicinity of the QCP ($x = 0.7$), on the nonmagnetic side of the phase diagram, the resonance assumes a character where the relaxation is via a single s-like band. The effective exchange interaction parameter J_{fs} in this compound is, within experimental errors, the same as at $x = 0.5$ but no local f-like electrons are probed by the Gd^{3+}, only the KLP. Further increase in the Sn substitution do not alter the Gd^{3+} resonance process of relaxation, which remains being via a single s-like ce band. For $x = 1.5$ the exchange interaction is q dependent, indicating that it is not isotropic over the FS and this dependance might be related with an anisotropy observed in the s-f hybridization for $CeIn_1Sn_2$ [29]. In $CeSn_3$ the J_{fs} value decreases slightly compared to $CeIn_{1.55}Sn_{1.45}$ probably due to intermediate valence effects and/or lattice expansion. So, once the system crosses the QCP the hybridization of the localized $4f$ electrons with the ce band becomes a global process and it condenses only into the KLP, $f(T/T^*) = 1$. Fig. 2(c) summarizes qualitatively this discussion of the Gd^{3+} ESR evolution in the $CeIn_{3-x}Sn_x$ materials.

Despite being difficult to assert on whether the QCP in $CeIn_{3-x}Sn_x$ is of the itinerant or localized scenario, it is important to notice that there are still some local moments very close to the QCP on the AFM state and none in its vicinity. This suggests it may be more in accordance with a local class of QCP, consistent with 2D AFM magnetic fluctuations [2, 12, 13].

In summary, our ESR results microscopically show that the $CeIn_{3-x}Sn_x$ system can be described by the two-fluid model for HF in the vicinity of the QCP. Also that the Ce $4f$ electrons present a localized component until very close to the QCP, in the magnetically ordered phase, indicating it might have a local character as in the P-driven QCP in $CeIn_3$.

We thank J. C. B. Monteiro and F. C. G. Gandra for the help with the polycrystalline samples. This work was supported by FAPESP, CNPq and CAPES (Brazil).

---

[*] Electronic address: eduardo.bittar@lnls.br

[1] G.R. Stewart, Rev. Mod. Phys. **56**, 755 (1984).
[2] H.v.Löhneysen *et al.*, Rev. Mod. Phys. **79**, 1015 (2007).
[3] S. Nakatsuji *et al.*, Phys. Rev. Lett. **89**, 106402 (2002).
[4] S. Nakatsuji *et al.*, Phys. Rev. Lett. **92**, 016401 (2004).
[5] Y.F. Yang *et al.*, Phys. Rev. Lett. **100**, 096404 (2008).
[6] Y.F. Yang *et al.*, Nature **454**, 611 (2008).

[7] N.J. Curro *et al.*, Phys. Rev. B **70**, 235117 (2004).
[8] H. Martinho *et al.*, Phys. Rev. B **75**, 045108 (2007).
[9] J.M. Lawrence, Phys. Rev. B **20**, 3770 (1979).
[10] P. Pedrazzini *et al.*, Eur. Phys. J. B **38**, 445 (2004).
[11] N.D. Mathur *et al.*, Nature **394**, 39 (1998).
[12] N. Berry *et al.*, Phys. Rev. B **81**, 174413 (2010).
[13] R. Küchler *et al.*, Phys. Rev. Lett. **96**, 256403 (2006).
[14] A.V. Silhanek *et al.*, Phys. Rev. Lett. **96**, 206401 (2006).
[15] R. Settai *et al.*, J. Phys. Soc. Jpn. **74**, 3016 (2005).
[16] S. Kawasaki *et al.*, Phys. Rev. B **77**, 064508 (2008).
[17] E.M. Bittar *et al.*, arXiv 1107.2587.
[18] See supplemental material at [?].
[19] T. Gambke *et al.*, Phys. Rev. Lett. **40**, 1290 (1978).
[20] J.G.S. Duque *et al.*, Phys. Rev. B **76**, 125114 (2007).
[21] E.M. Bittar *et al.*, Physica B **404**, 2995 (2009).
[22] C. Rettori *et al.*, Phys. Rev. B **10**, 1826 (1974).
[23] S.E. Barnes, Adv. Phys. **30**, 801 (1981).
[24] D. Davidov *et al.*, Solid State Commun. **12**, 621 (1973).
[25] R.R. Urbano *et al.*, Phys. Rev. B **75**, 045107 (2007).
[26] J.W.M. Pinto and H.O. Frota, Phys. Rev. B **64**, 092404 (2001).
[27] T. Gambke and B. Elschner, J. de Phys. Colloques **40**, C5-331 (1979).
[28] A.M. Toxen *et al.*, Phys. Rev. B **8**, 90 (1973).
[29] A.P. Murani *et al.*, Phys. Rev. Lett. **101**, 206405 (2008).

PROBING THE TWO-FLUID BEHAVIOR IN $\mathbf{CeIn_{3-x}Sn_x}$ BY ELECTRON SPIN RESONANCE (SUPPLEMENTAL MATERIAL)

In this supplemental material we first present the experimental details of our study. Secondly we show in more detail the calculations of the Gd^{3+} effective exchange interaction parameter for each compound grown in the $CeIn_{3-x}Sn_x$ series presented in the main text, which we start with a brief discussion on the theory of electron spin resonance (ESR) in metals. Detailed information on the theory can be found in the reviews articles listed in Refs. 1 and 2.

EXPERIMENTAL DETAILS

Single crystals of Gd doped $CeIn_{3-x}Sn_x$ are synthesized by the flux-growth technique. Elemental Ce:Gd:In:Sn are weighted in the ratio 1-y:y:10-$(10x/3)$:$10x/3$, with a nominal value for y of 0.005 and $x = 0$, 1.5 and 3. Polycrystalline samples are also grown by arc melting in Argon atmosphere. In this case the reactants ratio used is 1-y:y:3-x:x, with the same nominal value for y and $x = 0$, 0.5, 0.7, 1.5 and 3. X-ray powder diffraction measurements confirm the cubic $AuCu_3$ (Pm-$3m$) type structure for all synthesized compounds. The temperature dependence of the magnetic susceptibility, $\chi(T)$, is measured for $2 \leq T \leq 300$ K, after zero field cooling (ZFC). All ESR experiments are performed on a fine powder ($d \leq 38$ μm) in a Bruker ELEXSYS X-band spectrometer (9.4 GHz) with a TE_{102} cavity coupled to a helium-gas-flux T-controller system for $4.2 \leq T \leq 300$ K. Fine powder of crushed single crystals are used in the ESR experiments in order to increase the ESR signal-to-noise ratio.

The actual Sn concentrations are obtained from the cubic lattice parameter in which one expects it follows a linear increase (Vegard law) [3] (see Supplemental Figure 1(a)). For $x = 3$ the departure of linear behavior is due to the Ce ions intermediate valence effects for $x \gtrsim 2.2$ [4]. The T-dependence of the magnetic susceptibility $\chi(T)$ for the series of compounds $Ce_{1-y}Gd_yIn_{3-x}Sn_x$, corrected for the core diamagnetism, is shown in Supplemental Figure 1(b). From the Curie-Weiss law fitting of the low-T data the actual Gd doping concentration is obtained.

$\mathbf{Gd^{3+}}$ EFFECTIVE EXCHANGE INTERACTION PARAMETER CALCULATIONS IN $\mathbf{CeIn_{3-x}Sn_x}$

$\mathbf{Gd^{3+}}$ ESR in metals

In the simplest treatment of the exchange interaction $J_{fs}(q)\mathbf{S}\cdot\mathbf{s}$ between a localized $4f$ electron spin ($\mathbf{S}$) on a solute atom (Gd^{3+}) and the free conduction electron

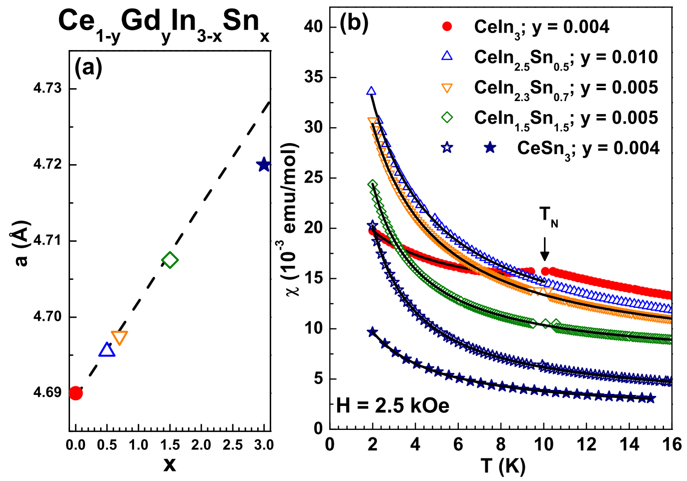

Supplemental FIG 1: Gd^{3+} in $Ce_{1-y}Gd_yIn_{3-x}Sn_x$: (a) cubic lattice parameter a dependance as a function of x. The dashed line represents the Vegard law [3]. For $x = 3$ the departure of linear behavior is due to the Ce ions intermediate valence effects for $x \gtrsim 2.2$ [4]. (b) Low-T dependence of $\chi(T)$ at H = 2.5 kOe. The solid lines are the Curie-Weiss fitting. The closed symbols identify the single crystalline samples and the open ones the polycrystals.

spin ($\mathbf{s}$) of the host metal, the ESR g shift Δg (Knight shift) [5] and the thermal broadening of the linewidth b (Korringa rate) [6] can be written as:

$$\Delta g = J_{fs}(0)\eta_{F_s}, \tag{3}$$

and

$$b = \frac{d(\Delta H)}{dT} = \frac{\pi k_B}{g\mu_B} J_{fs}(0)^2 \eta_{F_s}^2, \tag{4}$$

where $J_{fs}(0)$ is the effective exchange interaction parameter between the Gd^{3+} f local moment and the s-like conduction electron in the absence of conduction electron momentum transfer ($q = |\mathbf{k} - \mathbf{k}'| = k_F[2(1 - cos\theta_{\mathbf{k}\mathbf{k}'})]^{1/2} = 0$) [8]. $\eta(F_s)$ is the s-like band bare density of states for one spin direction at the Fermi surface. The constants k_B, μ_B and g are the Boltzman constant, the Bohr magneton and the Gd^{3+} g value in insulators ($g = 1.993$), respectively. The constant $\pi k_B/g\mu_B$ is 2.34×10^4 Oe/K in CGS units.

Equations 3 and 4 are normally used in the analysis of the ESR data for highly diluted rare-earths magnetic moments in intermetallic compounds with appreciable residual resistivity, i.e., large conduction electron spin-flip scattering (absence of "bottleneck" and "dynamic" effects) [7]. Since in our study we find that the ESR parameters are independent of the concentration, we can assume that the system is in the unbottleneck regime [7]. Combining the above equations we can write:

$$b = \frac{\pi k_B}{g\mu_B}(\Delta g)^2. \tag{5}$$

Sometimes the effective exchange interaction constant is not independent of the momentum transfer ($q \neq 0$) and in this more general case, Eq. 4 has to be rewritten as:

$$b = \frac{\pi k_B}{g\mu_B}\left\langle J_{fs}^2(q)\right\rangle \eta_{F_s}^2, \tag{6}$$

or alternatively, using Eq. 3:

$$b = \frac{\pi k_B}{g\mu_B}\frac{\left\langle J_{fs}^2(q)\right\rangle_F}{J_{fs}^2(0)}\Delta g^2, \tag{7}$$

where $\langle J_{fs}^2(q)\rangle_F$ is the square of the effective exchange interaction parameter in the presence of conduction electrons momentum transfer, averaged over the Fermi surface [8].

The g shift is due to the polarization of the conduction electrons by the localized magnetic moment and measures the exchange interaction parameter J_{fs} in the absence of conduction electrons momentum transfer ($q = 0$). On the other hand, the Korringa rate measures the averaged exchange interaction constant $\langle J_{fs}^2(q)\rangle_F$ over the Fermi surface ($0 \leq q \leq 2k_F$) [1]. So if $\langle J_{fs}^2(q)\rangle_F^{1/2} = J_{fs}$ (no momentum transfer) the ESR evolution is governed by Eqs. 3 and 4. Otherwise, if $\langle J_{fs}^2(q)\rangle_F^{1/2} \neq J_{fs}$ (q dependance) the resonance is described by Eqs. 3 and 6.

One way to know if the system is momentum transfer dependent is to analyze Eq. 5. If the calculated Korringa rate b_{cal} by the experimental Δg gives an equal value of the experimental Korringa rate b_{exp} ($b_{cal} = b_{exp}$) q dependance can be neglected. However, if $b_{cal} > b_{exp}$ then it can not. This is because $\langle J_{fs}^2(q)\rangle_F / J_{fs}^2(0) \leq 1$, being equal to 1 only when $\langle J_{fs}^2(q)\rangle_F^{1/2} = J_{fs}$.

Until now we have considered the that the resonance relaxes to a conduction band solely by a s-like band. However there might be cases where the conduction band has also d-, p- or f-like electrons. In this case Eqs. 3 and 4 are not valid. Differently than what happens with q dependent systems, multiband ESR gives $b_{cal} \ll b_{exp}$ by using experimental Δg in Eq. 5. Thus, Eqs. 3 and 4 must be rewritten, respectively as:

$$\begin{aligned} \Delta g &= \Delta g_{fs} + \Delta g_{fd} + \Delta g_{fp} + \ldots \\ &= J_{fs}\eta_{F_s} + J_{fd}\eta_{F_d} + J_{fp}\eta_{F_p} + \ldots \end{aligned} \tag{8}$$

and

$$b = \frac{\pi k_B}{g\mu_B}J_{fs}^2\eta_{F_s}^2 + \frac{\pi k_B}{g\mu_B}J_{fd}^2\eta_{F_d}^2 + \frac{\pi k_B}{g\mu_B}J_{fp}^2\eta_{F_p}^2 + \ldots, \tag{9}$$

where J_{fs}, J_{fd} e J_{fp} are the exchange interaction constant between the Gd^{3+} $4f$ spin and the s-, d- and p-like bands, respectively. η_{F_s}, η_{F_d} and η_{F_p} are the bare density of states for one spin direction at the Fermi surface for each respective band.

The exchange interaction parameter signal is positive for atomic interaction , i.e., ferromagnetic interactions, and negative for covalent mixing, antiferromagnetic-like. So it is straightforward to see why multiband enhances the Korringa rate compared to b_{cal}, since the dependance of the Korringa rate is quadratic with the exchange interaction parameters and it is always a sum. While for Δg it is linear and depends on the sign and strength of each exchange interaction constant. Therefore, the Δg sign can give valuable information about the interaction between the localized moment and its environment.

In the $\mathrm{CeIn}_{3-x}\mathrm{Sn}_x$ system, J_{fs} and J_{fd} are positives and J_{fp} and J_{ff} negatives [1].

Calculations

We now turn to the detailed calculations of the analysis of the Gd^{3+} ESR data in the $\mathrm{Ce}_{1-y}\mathrm{Gd}_y\mathrm{In}_{3-x}\mathrm{Sn}_x$ compounds. Supplemental Table III summarizes the experimental parameters found by ESR.

Supplemental TABLE III: Experimental parameters for Gd^{3+} diluted in $\mathrm{Ce}_{1-y}\mathrm{Gd}_y\mathrm{In}_{3-x}\mathrm{Sn}_x$. The values of γ are taken from Ref. 3.

Gd^{3+}	Gd		H_0	b	γ
in	y	Δg	[Oe]	[Oe/K]	[mJ/mol K^2]
CeIn_3	0.004	-0.023(5)	120(5)	0.1(1)	130
$\mathrm{CeIn}_{2.5}\mathrm{Sn}_{0.5}$	0.010	+0.007(10)	825(45)	38(3)	730(50)
$\mathrm{CeIn}_{2.3}\mathrm{Sn}_{0.7}$	0.005	+0.027(10)	820(25)	15(5)	750(50)
$\mathrm{CeIn}_{1.5}\mathrm{Sn}_{1.5}$	0.005	+0.140(10)	650(60)	30(5)	250(20)
CeSn_3	0.004	+0.027(5)	150(5)	16(1)	73

Calculation for $x = 0.0$

For Gd^{3+} in CeIn_3 we find experimentally $\Delta g \simeq -23(5) \times 10^{-3}$ and $b = 0.1(1)$ Oe/K. Using Eq. 5 and $\Delta g \simeq -23(5) \times 10^{-3}$, knowing that $\pi k_B / g\mu_B = 2.34 \times 10^4$ Oe/K one expects $b \approx 12(5)$ Oe/K. This value is much larger than the measured experimentally $b = 0.1(1)$ Oe/K. Therefore, we conclude that the approximations made in Eqs. 3 and 4 are not adequate. To account for a Δg negative value, contributions coming from the exchange interaction with p- or f-like ce bands, that have opposite signs, must take place in the relaxation process [1]. However, multiple bands enhances the Korringa rate, which is not the case of Gd^{3+} in CeIn_3, where there is indication of q dependance of the effective exchange interaction parameter since $b_{cal} \gg b_{exp}$. From the considerations stated in the main text we can assume that the exchange interaction of the Gd^{3+} is only with f-like conduction electrons. Because J_{ff} is negative it accounts for $\Delta g < 0$ (Eq. 3). However, the experimental Korringa rate is much smaller than the calculated one using experimental Δg, indicating a q dependent effective exchange interaction. We then can rewrite Eqs. 3 and 6 respectively as:

$$\Delta g = J_{ff}(0)\eta_{F_f} \tag{10}$$

and

$$b = \frac{\pi k_B}{g\mu_B} \left\langle J_{ff}^2(q) \right\rangle_F \eta_{F_f}^2 . \tag{11}$$

In the free conduction electron gas model, the electronic heat capacity or Sommerfeld coefficient γ is given by:

$$\gamma = (2/3)\pi^2 k_B^2 \eta_F \tag{12}$$

and one can obtain, using its experimental value, the bare density of states for one spin direction at the Fermi surface.

For CeIn_3 $\gamma^{x=0} = 130$ mJ/(mol K^2) [3], so we get from Eq. 12 $\eta_F^{x=0} = 28(2)$ states/(eV mol spin). Assuming that in this compound the density of states at the Fermi level for the $4f$ electrons $\eta_{F_f}^{x=0}$ is:

$$\eta_{F_f}^{x=0} = \eta_F^{x=0} - \eta_F^{LaIn_3},$$

where $\eta_F^{LaIn_3} = 0.8(1)$ states/(eV mol spin) (see Fig. 4 of Ref. 9), we calculate $\eta_{F_f}^{x=0} = 27(2)$ states/(eV mol spin).

Using Eqs. 10 and 11 and experimental values of Δg and b, and $\eta_{F_f}^{x=0} = 27(2)$ states/(eV mol spin) we obtain $J_{ff}(0) = -0.8(1)$ meV and $\langle J_{ff}^2(q) \rangle_F^{1/2} = 0.07(1)$ meV.

Calculation for $x = 0.5$

For Gd^{3+} in $\mathrm{CeIn}_{2.5}\mathrm{Sn}_{0.5}$ we find experimentally $\Delta g \simeq 4(10) \times 10^{-3}$ and $b = 38(3)$ Oe/K. Using Eq. 5 and $\Delta g \simeq 7(10) \times 10^{-3}$ one expects $b \approx 1$ Oe/K. Since $b_{cal} \ll b_{exp}$ multiband effects are present and no q dependance is seen. As the main text points out, for this compound contribution of the Ce^{3+} $4f$ itinerant s- and localized f-like conduction electrons bands take place in the Gd^{3+} resonance relaxation process. In this case Eqs. 8 and 9 can be rewritten respectively as:

$$\Delta g = J_{fs}\eta_{F_f^{it}} + J_{ff}\eta_{F_f^{loc}} \tag{13}$$

and

$$b = \frac{\pi k_B}{g\mu_B} \left[J_{fs}^2 \eta_{F_f^{it}}^2 + J_{ff}^2 \eta_{F_f^{loc}}^2 \right], \tag{14}$$

where $\eta_{F_f^{it}}$ and $\eta_{F_f^{loc}}$ are the band bare density of states for one spin direction at the Fermi surface for the itinerant- and localized-like conduction electron band, respectively.

From $\gamma^{x=0.5} = 730(50)$ mJ/(mol K^2) [3] and Eq. 12 we get $\eta_F^{x=0.5} = 155(2)$ states/(eV mol spin). Assuming that:

$$\eta_{F_f}^{x=0.5} = \eta_F^{x=0.5} - \eta_F^{LaIn_{2.5}Sn_{0.5}},$$

where $\eta_F^{LaIn_{2.5}Sn_{0.5}} = 0.8(1)$ states/(eV mol spin) (see Fig. 4 of Ref. 9), we calculate $\eta_{F_f}^{x=0.5} = 154(2)$ states/(eV mol spin).

Solving the system of three equations below for $\eta_{F_f}^{x=0.5} = 154(2)$ states/(eV mol spin), $\Delta g \simeq 7(10)\times 10^{-3}$, $b = 38(3)$ Oe/K and $J_{ff}^{x=0.5} = J_{ff}^{x=0} = 0.0008$ eV:

$$\eta_{F_f}^{x=0.5} = \eta_{F_f^{it}} + \eta_{F_f^{loc}} = 154,$$

$$\Delta g = J_{fs}\eta_{F_f^{it}} + 0.0008 \cdot \eta_{F_f^{loc}} = 7 \times 10^{-3}$$

and

$$b = 2.34 \times 10^4 \cdot \left[J_{fs}^2 \eta_{F_f^{it}}^2 + (0.0008)^2 \cdot \eta_{F_f^{loc}}^2\right] = 38,$$

we obtain $J_{fs} = 0.3(1)$ meV, $\eta_{F_f^{it}} = 115(10)$ states/(eV mol spin) and $\eta_{F_f^{loc}} = 40(5)$ states/(eV mol spin).

Calculation for $x = 0.7$

For Gd^{3+} in CeIn$_{2.3}$Sn$_{0.7}$ we find experimentally $\Delta g \simeq 27(10) \times 10^{-3}$ and $b = 15(5)$ Oe/K. Using Eq. 5 and $\Delta g \simeq 27(10) \times 10^{-3}$ one expects $b \approx 17(10)$ Oe/K. For this case, approximations made in Eqs. 3 and 4 are in fact adequate, once $b_{cal} \approx b_{exp}$.

From $\gamma^{x=0.7} = 750(50)$ mJ/(mol K^2) [3] and Eq. 12 we get $\eta_F^{x=0.7} = 160(10)$ states/(eV mol spin). Using Eq. 4:

$$b = 2.34 \times 10^4 \cdot J_{fs}(0)^2 \cdot (160)^2 = 15,$$

we find $J_{fs} = 0.2(1)$ meV, similar to value encountered for $x = 0.5$.

Calculation for $x = 1.5$

For Gd^{3+} in CeIn$_{1.5}$Sn$_{1.5}$ we find experimentally $\Delta g \simeq 140(10) \times 10^{-3}$ and $b = 30(5)$ Oe/K. The Δg value observed in Ce$_{0.995}$Gd$_{0.005}$In$_{1.5}$Sn$_{1.5}$ relates to a Korringa rate $b \simeq 500(100)$ Oe/K by Eq. 5 ($b_{cal} \gg b_{exp}$). So in this case $\langle J_{fs}^2(q)\rangle_F^{1/2} \neq J_{fs}$ because of a q dependent effective exchange interaction.

From $\gamma^{x=1.5} = 250(20)$ mJ/(mol K^2) [3] and Eq. 12 we get $\eta_F^{x=1.5} = 53(4)$ states/(eV mol spin). Using Eqs. 3 and 6, respectively:

$$\Delta g = J_{fs}(0) \cdot 53 = 140(10) \times 10^{-3},$$

and

$$b = 2.34 \times 10^4 \cdot \left\langle J_{fs}^2(q)\right\rangle \cdot (53)^2 = 30,$$

we calculate $J_{fs}(0) = 2.6(2)$ meV and $\langle J_{fs}^2(q)\rangle_F^{1/2} = 0.7(1)$ meV.

Calculation for $x = 3.0$

For Gd^{3+} in CeSn$_3$ we find experimentally $\Delta g \simeq 27(5) \times 10^{-3}$ and $b = 15(1)$ Oe/K. From Eq. 5, we get $b \approx 17(5)$ Oe/K, very close to the experimental value, i.e., multiband and q dependance effects of the exchange interaction may be neglected.

From $\gamma^{x=3} = 73$ mJ/(mol K^2) [3] and Eq. 12 we get $\eta_F^{x=3} = 16(1)$ states/(eV mol spin). Using Eq. 4:

$$b = 2.34 \times 10^4 \cdot J_{fs}(0)^2 \cdot (16)^2 = 15,$$

we find $J_{fs} = 1.7(1)$ meV.

---

[*] Electronic address: eduardo.bittar@lnls.br

[1] S.E. Barnes, Adv. Phys. **30**, 801 (1981).
[2] R.H. Taylor, Adv. Phys. **24**, 681 (1975).
[3] P. Pedrazzini, M.G. Berisso, N. Caroca-Canales, M. Deppe, C. Geibel, and J.G. Sereni, Eur. Phys. J. B **38**, 445 (2004).
[4] J.M. Lawrence, Phys. Rev. B **20**, 3770 (1979).
[5] K. Yosida, Phys. Rev. **106**, 893 (1957).
[6] J. Korringa, Physica **16**, 601 (1950).
[7] C. Rettori, H.M. Kim, E.P. Chock, and D. Davidov, Phys. Rev. B **10**, 1826 (1974).
[8] D. Davidov, K. Maki, R. Orbach, C. Rettori, and E.P. Chock, Solid State Commun. **12**, 621 (1973).
[9] A.M. Toxen, R.J. Gambino, and L.B. Welsh, Phys. Rev. B **8**, 90 (1973).